



UNIVERSITY OF LEEDS

This is a repository copy of *Detection of a persistent meteoric metal layer in the Martian atmosphere*.

White Rose Research Online URL for this paper:
<http://eprints.whiterose.ac.uk/115647/>

Version: Accepted Version

Article:

Cristmani, MMJ, Schneider, NM, Plane, JMC orcid.org/0000-0003-3648-6893 et al. (13 more authors) (2017) Detection of a persistent meteoric metal layer in the Martian atmosphere. *Nature Geoscience*, 10 (6). pp. 401-404. ISSN 1752-0894

<https://doi.org/10.1038/ngeo2958>

© 2016 Macmillan Publishers Limited. All rights reserved. This is an author produced version of a paper published in *Nature Geoscience*. Uploaded in accordance with the publisher's self-archiving policy.

Reuse

Items deposited in White Rose Research Online are protected by copyright, with all rights reserved unless indicated otherwise. They may be downloaded and/or printed for private study, or other acts as permitted by national copyright laws. The publisher or other rights holders may allow further reproduction and re-use of the full text version. This is indicated by the licence information on the White Rose Research Online record for the item.

Takedown

If you consider content in White Rose Research Online to be in breach of UK law, please notify us by emailing eprints@whiterose.ac.uk including the URL of the record and the reason for the withdrawal request.



eprints@whiterose.ac.uk
<https://eprints.whiterose.ac.uk/>

Detection of a persistent meteoric metal layer in the Martian atmosphere

M. M. J. Crismani¹, N. M. Schneider¹, J. M. C. Plane², J. S. Evans³, S. K. Jain¹, M. S. Chaffin¹, J. D. Carrillo-Sanchez², J. I. Deighan¹, R. V. Yelle⁴, A. I. F. Stewart¹, W. McClintock¹, J. Clarke⁵, G. M. Holsclaw¹, A. Stiepen⁶, F. Montmessin⁷, & B. M. Jakosky¹

1 Laboratory for Atmospheric and Space Physics (LASP), University of Colorado, USA,

2 School of Chemistry, University of Leeds, Leeds, UK

3 Computational Physics, Inc., Springfield, Virginia, USA

4 Lunar and Planetary Laboratory, University of Arizona, Tucson, Arizona, USA

5 Center for Space Physics, Boston University, Boston, MA, USA,

6 Laboratoire de Physique Atmosphérique et Planétaire, Space sciences, Technologies and Astrophysics Research (STAR)

7 LATMOS/IPSL, Guyancourt, France

Interplanetary dust particles sporadically enter planetary atmospheres at orbital velocities and ablate as collisions occur with ambient gases to produce a persistent layer of metallic atoms (e.g. Fe, Mg, Na) in their upper atmospheres. Such layers are well studied at Earth, but have not been directly detected elsewhere in the Solar System. Here we report the detection of a meteoric layer consisting of Mg⁺ ions near an altitude of 90 km in the Martian atmosphere from ultraviolet remote sensing observations by NASA's MAVEN spacecraft. We observe temporal variability in the Mg⁺ layer over the course of a Martian year, moving up and down in altitude seasonally and in response to dust storms, and displaying diurnal fluctuations in density. We also find that most meteor showers do not significantly perturb this layer, which constrains the fluence of eleven observed Martian meteor showers to less than our estimated global dust flux. The persistence and variability of the Mg⁺ layer are difficult to explain with existing models and reconcile with other transient layers of ions observed in the Martian ionosphere. We suggest that

the transient layers are not sourced from the persistent Mg⁺ layer and thus not derived from meteoric material, but are ambient ions produced by some unknown mechanism.

High-speed collisions with air molecules cause rapid heating of interplanetary dust particles (IDPs), melting and evaporating their constituent minerals^{1,2,3}. This ablation process deposits a variety of atomic constituents at the ~1 μbar level (80-110 km on Earth). Non-volatile elements such as Mg, Fe and Na act as direct tracers of the ablation process, as no other processes transport these species to these altitudes. These elements are in approximate equilibrium between supply through ablation⁴ and loss by chemical reactions forming oxides, hydroxides, and carbonates, which subsequently polymerize into particles called meteoric smoke⁵. Meteoric smoke particles most likely provide condensation nuclei for high altitude CO₂ ice clouds at Mars⁶. In addition to the quasi-steady-state supply from random (or “sporadic”) meteors, the ablation of cometary dust during meteor showers can supply additional metals to the upper atmosphere.

The Mars Atmosphere and Volatile EvolutionN (MAVEN) mission was designed to study the response of Mars’ upper atmosphere to solar influences⁷, which also renders it capable of detecting the influence of IDPs. This capability was clearly demonstrated during the exceptionally close pass of comet C/2013 A1 (Siding Spring) by Mars in 2014, and the ensuing meteor shower^{8,9,10,11}. Of the many elements that ablate from IDPs, Mg⁺ and Mg are most readily detectable in ultraviolet (UV) remote sensing, and were observed in a transient layer after the passage of comet Siding Spring¹¹. The other dominant species by mass, Fe and Na, are not observed by IUVS due to their reduced

scattering efficiencies in the UV¹². Here we report on remote sensing observations of Mg⁺ over the course of MAVEN's two-year mission that are consistent with a persistent meteoric layer.

MAVEN's remote sensing instrument for studying Mars' upper atmosphere is the Imaging Ultraviolet Spectrograph (IUVS)¹³. This instrument observes in the far and middle UV (110-190 nm and 190-340 nm) in separate channels, and measures atmospheric emissions from CO₂, its dissociation and ionization products as well as atomic and molecular species such as O and N₂^{14,15}. The instrument uses a scan mirror to construct vertical profiles of emergent radiation from the atmosphere at the limb. We use observations from the periapse segment of each orbit, where IUVS produces limb scans over the altitude range 75-250 km. During each orbit, IUVS takes up to 12 limb scans in a ~22 minute observation period spanning ~45 degrees around the planet. MAVEN's elliptical orbit precesses about Mars on timescales of months to provide complete coverage of the planet. Data processing techniques are outlined in detail in previous MAVEN/IUVS papers^{11,14,15,16,17} and all data used herein are available on the NASA Planetary Data System.

Detection and Variability of Mg⁺

Emission from Mg⁺ was reliably detected in every periapse limb scan obtained over one Mars year (two Earth years; Figures 1, 3) whenever the Mg⁺ layer was appropriately illuminated and the instrument orientation did not introduce excessive scattered solar continuum (for these purposes, stray light). The Mg⁺ emission feature, centered on 280 nm, is due to resonant scattering of solar UV photons rather than direct excitation during ablation. Mg⁺ brightnesses were extracted from a model spectrum fit

(Figure 1a,b), using line positions and atomic constants of known emitters in this spectral region plus a stray light solar spectrum ^{15,16,18}.

The Mg⁺ emission brightness was converted to local ion density through an Abel transform, common in the study of optically thin airglow emissions ¹⁹ (see SI). The Mg⁺ layer has a mean peak concentration of $\sim 250 \text{ cm}^{-3}$ and is typically found near an altitude of 90 km (Figure 2). Reported altitudes carry a 2.5 km uncertainty consistent with slit averaging in 5 km bins ¹⁶. Figure 3 shows the derived densities in a fixed altitude range over the course of the mission. Brightness measurements carry Poisson random uncertainties propagated through a multiple linear regression technique and Abel transform. In addition, the brightnesses are subject to 30% systematic uncertainty in absolute calibration (not shown in figure error sizes) ¹⁴. The random and systematic uncertainties propagate linearly into densities and other derived quantities.

Observations of Mg⁺ density demonstrate real variability (Figure 3) beyond the random uncertainties. First, the lower atmosphere of Mars warms and cools seasonally and in response to dust storms, moving the ablation layer up and down relative to the fixed altitude range used here ²⁰. Second, the Mg⁺ density decreases by up to factor of ~ 5 towards the dawn and dusk terminators. This effect is most pronounced near the equator and less noticeable near the poles where the diurnal cycle decreases in intensity.

The Lack of Mg Challenges Existing Models

Emission from atomic Mg has only been reliably detected (Figure 1b) during the exceptionally intense meteor shower of comet Siding Spring ¹¹. Scaling Mg⁺ by the ratio of the Mg and Mg⁺ scattering efficiencies at our most marginal detection, we find that IUVS would have detected atomic Mg at concentrations greater than 130 cm^{-3} . This value

falls well below the concentration predicted based on our existing understanding of ablation and atmospheric chemistry (Figure 2).

The apparent absence of neutral Mg therefore poses a significant challenge to our understanding of the chemical reactions that create and connect Mg and Mg⁺. Laboratory studies validated by terrestrial observations⁶ have been incorporated in the Chemical Ablation MODel (CABMOD)^{21,22} which describes the ablation physics and chemistry, and is coupled to a 1-D atmospheric model which tracks subsequent atmospheric chemistry (see the SI for further details). When adapted for conditions at Mars, CABMOD predicts that Mg atoms would be injected directly during ablation and should build a neutral Mg layer below 100 km. Mg⁺ would then be produced through charge exchange with ambient O₂⁺²². Atomic Mg would also undergo a series of reactions to create a steady-state population of MgCO₃. Together these reactions are expected to yield an Mg/Mg⁺ ratio of ~4 at 90 km, contrary to the observed upper limit of ~0.5. Furthermore, at 90 km Mg⁺ should have a lifetime comparable to a Mars day²¹ and should therefore exhibit negligible diurnal variation.

Alternative chemical pathways were investigated to explore the relationship between Mg and Mg⁺. In particular, if the dissociative recombination of MgCO₃⁺ with electrons yields MgO rather than Mg, then the Mg layer would remain below the IUVS detection limit. (Both the baseline and alternate 1-D model results are described more fully in the Supplemental Information.) Additional laboratory studies are needed to accurately determine the branching ratio, and whether other unknown chemistry plays a role. Ongoing efforts to examine the evolution of metallic species following the Siding Spring encounter will appear in a subsequent publication; this period provides the only

observed ratios of Mg and Mg⁺, and may further constrain this chemistry. None of the alternative chemical reactions we explored provide an explanation for the strong diurnal variation in Mg⁺.

Constraining the Interplanetary Dust Flux at Mars

The IUVS measurements can be used to provide the first remote sensing estimate of IDP flux at a planet other than Earth. At Earth, the observed metal layer is supplied from the main IDP sources, Jupiter Family Comets, asteroids, and long-period comets (Halley Type and Oort Cloud), with particle mass ranging from 10⁻⁴ and 10⁻⁷ g, and a global input of 29 - 57 tonnes d⁻¹ ²³. We do not expect Mars' metal layer to be sourced from a different population, and these observations directly constrain the largest IDP population by mass (excluding surface impactors), making a direct measurement essential for an accurate estimate.

Mars' global dust input was estimated by comparing a Mars Zodiacal Dust Cloud derived model ²⁴ to representative profiles with local times near noon and where the peak and underside of the layer were clearly detectable. In the baseline chemical model ²¹, which neglects the absence of observed Mg, we find a global dust input rate of ~2 tonnes sol⁻¹; in the alternate model this value is ~3 tonnes sol⁻¹ (see the SI for details). Note that uncertainties in the MgCO₃⁺ chemistry render the 2 tonnes sol⁻¹ a lower limit, as alternative reactions to reduce the abundance of Mg also reduce the efficiency for creating Mg⁺. The instrument's systematic and observational uncertainties are small in comparison to this range in estimates, and therefore are omitted from this result. Comparing the dust environment at Mars to Earth, and accounting for their difference in

surface area, we find the fluence at Mars of 2 - 3 tonnes sol⁻¹ is at the lower end of the measurements scaled from Earth ³, 1.4 - 14 tonnes d⁻¹.

As at Earth, these Mars fluences can be compared to spaceborne dust detectors. The MAVEN Langmuir Probe and Waves (LPW) instrument measured high altitude dust particles between 10⁻¹¹-10⁻⁷ g and determined a fluence of these particles to be between 85 kg sol⁻¹ and 8.5 tonnes sol⁻¹ ²⁵. Their extrapolation to the total input is necessarily imprecise due to the small masses sampled, which is not representative of the mass of IDPs that ablate and inject metals into the atmosphere. The Neutral Gas and Ion Mass Spectrometer (NGIMS) on MAVEN can also sample ablated metals ²⁶, though the region sampled lies several scale heights above the main deposition layer such that global fluence may not be possible to estimate.

Mars likely encounters regular meteor showers, analogous to Earth; however, we have been unable to detect any showers other than comet Siding Spring ¹¹, which produced Mg⁺ concentrations at 120 km between 5 x 10³ and 3 x 10⁴ cm⁻³. Of the 24 predicted Mars meteor showers since MAVEN's arrival at Mars, IUVS can constrain 11 of these events (Table S2) when it was observing in daylight and taking data. The Mg⁺ profiles at these times show no correlated increases ≥ 500 cm⁻³ (twice the mean), constraining the fluence of these showers to levels lower than the nominal global input of 3 tonnes sol⁻¹. Thus, the two-year timeline of meteoric metal layer observations reported here demonstrate that the observed meteor showers do not significantly perturb metal ion abundances. This result is similar to the Earth, where showers have not been conclusively shown to increase its metallic ion content ²⁷.

The observation timeline also argues strongly against a meteoric cause for transient ionospheric layers (the “M3 layer”) detected in radio occultation measurements²⁸. The M3 layer was detected in 1 - 10% of observations, with electron concentrations of 10^4 cm^{-3} . Although a meteoric origin was proposed, the nature of these electron concentrations is ambiguous because the M3 layer may be due to either an enhancement of meteoric (e.g. Mg^+ , the dominant ion from ablation) or ambient (O_2^+ , CO_2^+ etc.) ions. IUVS observations are performed in a similar geometry to radio occultations, and occur every ~ 4.5 hrs. Therefore, if the source of the M3 layer was metallic ions in concentrations approaching 10^4 cm^{-3} , the layer would be readily observed in 130-1300 profiles (Figure 3), whereas IUVS has not detected any Mg^+ densities larger than 10^3 cm^{-3} at any altitude outside of the comet Siding Spring epoch. Another origin, such as enhanced solar energetic particle precipitation or x-ray flux, may be responsible for the transient M3 layer.

References

- 1 Istomin, V. “Ions of extraterrestrial origin in the Earth atmosphere.” *Planetary and Space Science* **11**, 173–174 (1963)
- 2 Anderson, J, & Barth, C. “Rocket investigation of the Mg I and Mg II dayglow.” *J Geophys Res* **76**, 3723–3732 (1971)
- 3 Plane, J. “Cosmic dust in the earth’s atmosphere.” *Chem. Soc. Rev.* **41**, 6507–18 (2012)
- 4 Vondrak, T. et al. “A chemical model of meteoric ablation.” *Atmos. Chem. Phys.*, **8**, 7015–7031. (2008)
- 5 Plane, J., Feng, W. & Dawkins, E. “The mesosphere and metals: Chemistry and changes.” *Chemical reviews* **115**, 4497–4541 (2015)
- 6 Nachbar, M., Duft, D. & Mangan, T. “Laboratory measurements of heterogeneous CO₂ ice nucleation on nanoparticles under conditions relevant to the Martian mesosphere.” *J. Geophys. Res. Planets* **121**, 753–769 (2016)
- 7 Jakosky, B. et al. “The Mars Atmosphere and Volatile Evolution (MAVEN) Mission.” *Space Sci. Rev.* **195**, 3–48 (2015)
- 8 Benna, M. et al. “Metallic ions in the upper atmosphere of Mars from the passage of comet C/2013 A1 (Siding Spring).” *Geophys. Res. Lett.*, **42**, 4670–4675 (2015)
- 9 Gurnett, D. et al. “An ionized layer in the upper atmosphere of Mars caused by dust impacts from comet Siding Spring.” *Geophys. Res. Lett.*, **42**, 4745–4751 (2015)

- 10 Restano, M. et al. “Effects of the passage of Comet C/2013 A1 (Siding Spring) observed by the Shallow Radar (SHARAD) on Mars Reconnaissance Orbiter.” *Geophys. Res. Lett.*, **42**, 4663–4669 (2015)
- 11 Schneider, N. et al. “MAVEN IUVS observations of the aftermath of the Comet Siding Spring meteor shower on Mars.” *Geophys. Res. Lett.*, **42**, 4755–4761 (2015)
- 12 Kramida, A., Ralchenko, Y, Reader, J., & NIST ASD Team NIST Atomic Spectra Database (ver. 5.3), [Online] (2015)
- 13 McClintock, W. et al. “The Imaging Ultraviolet Spectrograph (IUVS) for the MAVEN Mission.” *Space Sci. Rev.* **195**, 75–124 (2015)
- 14 Evans, J. et al. “Retrieval of CO₂ and N₂ in the Martian thermosphere using dayglow observations by IUVS on MAVEN.” *Geophys. Res. Lett.*, **42**, 9040–9049 (2015)
- 15 Stevens, M. et al. “New observations of molecular nitrogen in the Martian upper atmosphere by IUVS on MAVEN.” *Geophys. Res. Lett.*, **42**, 9050–9056 (2015)
- 16 Jain, S. et al. “The structure and variability of Mars upper atmosphere as seen in MAVEN/IUVS dayglow observations.” *Geophys. Res. Lett.*, **42**, 9023–9030 (2015)
- 17 Crismani, M. et al. “Ultraviolet observations of the hydrogen coma of comet C/2013 A1 (Siding Spring) by MAVEN/IUVS.” *Geophys. Res. Lett.*, **42**, 8803–8809 (2015)
- 18 Dymond, K. et al. “Middle ultraviolet emission from ionized iron.” *Geophys. Res. Lett.*, **30.1**, 1003 (2003)

- 19 Chamberlain, J. & Hunten, D. "Theory of planetary atmospheres. An introduction to their physics and chemistry." Academic Press Inc. (1987)
- 20 Jakosky, B. et al. "Mars' atmospheric history derived from upper-atmosphere measurements of $^{38}\text{Ar}/^{36}\text{Ar}$." *Science* **355**, 1409-1410. (2017)
- 21 Whalley, C., & Plane, J. "Meteoric ion layers in the Martian atmosphere." *Faraday Discuss.* **147**, 349–368 (2010)
- 22 Molina-Cuberos, G., et al. "Meteoric ions in the atmosphere of Mars." *Planet Space Sci* **51**, 239–249 (2003)
- 23 Carrillo- Sánchez, J. et al. "Sources of Cosmic Dust in the Earth's Atmosphere." *Geophys. Res. Lett.*, **43** (2016)
- 24 Nesvorný, D. et al. "Cometary Origin of the Zodiacal Cloud and Carbonaceous Micrometeorites. Implications for Hot Debris Disks" *Astrophysical J* **713**, 816 (2010)
- 25 Andersson, L. et al. "Dust observations at orbital altitudes surrounding Mars." *Science* **350**, 6261 (2015)
- 26 Grebowsky, J. et al. "Unique, non-Earthlike, Meteoritic Ion Behavior in the Upper Atmosphere of Mars" Submitted to *Geophys. Res. Lett.* (2017)
- 27 Grebowsky, J. & Aikin A. "In Situ Measurements of Meteoric Ions" Cambridge University Press, (2002)
- 28 Pätzold, M. et al. "A Sporadic Third Layer in the Ionosphere of Mars." *Science* **310**, 837–839 (2005)

Acknowledgements

NASA supports the MAVEN mission through the Mars Scout program. M.M.J.C. would like to thank A. Christou and J. Vaubaillon for their input on the meteor shower candidate list and M. Slipski, P. Withers, and K. Peter for their insightful comments. J.M.C.P. is supported by the European Research Council (project 291332 - CODITA).

Corresponding Author

Please direct all questions, comments or inquiries to Matteo Crismani.

Author Contributions

M.M.J.C., S.K.J., J.S.E., J.D., and M.S.C. improved the data processing to create these data products. M.M.J.C., N.M.S., and J.M.C.P. developed the interpretation of this data. J.M.C.P. and J.D.C.S. created the model used herein. All authors contributed to the development of the instrument pipeline and/or data acquisition as well as interpretation and presentation of these results.

Competing Financial Interests

The authors declare no competing financial interests.

Figure 1 | Spectral identification of Mg⁺

This representative scan was taken near noon (10-15 hours local time) in the Northern hemisphere (50-70 N) on 4/22/16 (orbit 3040). **a**, The MUV spectrum is slit averaged and 1-sigma errorbars are propagated from the Poisson noise of the data. The data are shown as black circles, with known airglow emissions (see text) fit in blue. **b**, The residual (black line) from **a**, with an emission near 280 nm consistent with Mg⁺ (red) whose brightness is 1.81+/-0.13 kR. Atomic Mg has an emission feature at 285 nm whose predicted brightness (orange) is not detected (see Figure 2).

Figure 2 | Altitude Profile of Mg⁺ Compared to Model Predictions

IUVS derived Mg⁺ altitude profiles, averaged from orbit 3040 (the same data shown in Figure 1), compared with the baseline CABMOD prediction (see SI for model details). The predicted brightness is derived from the model density (Figure 2) using the atomic Mg scattering efficiency ², indicating (Figure 1b) that Mg is not detected despite large predicted concentrations.

Figure 3 | One Mars year of observations of Mg⁺.

Mg⁺ concentrations between 90-100 km over the course of ~two Earth years. The timeline omits the comet Siding Spring meteor shower of Oct 19th 2014, as the peak density of ~10⁵ is off-scale. Average measurement uncertainties are given for three densities in the legend. Observations taken at high solar zenith angle (darker colors, >70 deg) demonstrate marked reduction in Mg⁺, consistent with decreases toward the dawn and dusk terminators, especially near the equator. As observations sample a range of latitudes, these observations represent a variety of local time and latitude coverage. Blue diamonds indicate predicted meteor showers (see Table S2).

Methods

Mg⁺ Density Retrieval

To determine the density at the tangent point, we used an Abel transform method ¹⁸, considering the emission to be optically thin and a spherically symmetric observing geometry. Using the standard relationship for the scattering cross section, related to the oscillator strength and Doppler width ²⁹, we find the Mg⁺ doublet (at 140 K) cross section is 8.9 and 4.4 x 10⁻¹² cm². Therefore we do not expect self-scattering to become important until densities at the tangent point approach 10⁴ cm⁻³, and the path length is reduced to 100 km. As the retrieved densities are never larger than 10³ cm⁻³, we consider this emission optically thin, thus the Abel transform is a robust approximation to the density at the tangent point.

The g-factors for the Mg⁺ lines at 279.5528 and 280.2705 nm used herein are 10.05 x 10⁻² s⁻¹ and 4.64 x 10⁻² s⁻¹ respectively. Dymond ¹⁷ calculated 8.4 x 10⁻² s⁻¹ and 3.9 x 10⁻² s⁻¹, while Anderson and Barth ² calculated 9.1 x 10⁻² s⁻¹ and 3.7 x 10⁻² s⁻¹. Although Dymond cites their use of a higher resolution solar spectrum from A'Hearn et al. ³⁰, the spectrum found therein is actually not higher resolution, and a personally communicated spectrum from A'Hearn ³¹, which we used, may be instead what they were referencing. In this spectrum, the flux at 1 AU is 2.5 and 2.2 x 10¹² for 279.6 and 280.3 nm respectively. For the Mg line, we use the g-factor of Anderson and Barth ².

1-D Model Details

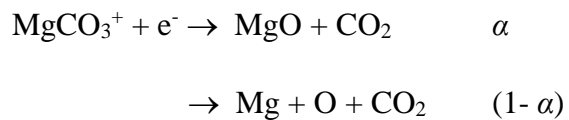
The 1-D model used for this study has been described in detail by Whalley and Plane ²⁰. The eddy diffusion coefficient (K_{zz}) profile in Figure S1 is taken from Rosenqvist and Chassefiere ³²: the value of $2 \times 10^6 \text{ cm}^2 \text{ s}^{-1}$ below 65 km was estimated from Phobos 2 solar occultation measurements of dust, ozone and clouds at low latitudes. The larger values ($> 10^7 \text{ cm}^2 \text{ s}^{-1}$) above 100 km are consistent with the K_{zz} required to model measurements made by the Viking 1 and 2 spacecraft ³³ and the values that have been used in other 1-D models ^{34,35}. The molecular diffusion coefficient profiles of Mg and Mg^+ are also illustrated in Figure S1, showing that the turbopause height is around 120 km - consistent with measurements made by the Neutral Gas Ion Mass Spectrometer (NGIMS) instrument on MAVEN ^{8, 25} during deep dip orbits down to 130 km.

The off-line sources of the vertical profiles of the minor trace species O_3 , O, O_2 , H, CO, O_2^+ , and electrons, for daytime low-latitude conditions, are described in Whalley and Plane ²⁰. Figure S2 compares the production rates of Mg^+ from photo-ionization and charge transfer with the major ambient O_2^+ ion, showing that charge transfer dominates between 90 and 190 km.

Table S1 contains rate coefficients for the reaction scheme used in the 1-D model. Most of these rate coefficients have now been measured over the temperature and pressure ranges needed to extrapolate with reasonable confidence to the conditions on Mars (see the footnotes to the Table). The rate coefficient for the reaction



was calculated using electronic structure theory to determine the reaction enthalpy (149 kJ mol⁻¹ at the cbs-qb3 level of theory) and molecular parameters, and then applying Rice-Ramsperger-Kassel-Markus (RRKM) theory³⁶. Dissociative recombination of the MgCO₃⁺ ion with an electron is assumed to have two reaction channels:



where α is the branching ratio.

Meteoric ablation is assumed to be the source of Mg species, and the Mg ablation profile peaking at ~80 km in the 1-D model of Whalley and Plane²⁰ was optimized to give agreement of the modeled and IUVS-measured peak of the Mg⁺ profile around 95 km.

The model was then run until steady-state conditions were reached (typically 20 days). The objective of the modeling was to explain the observed Mg⁺ profile, and the lack of a detectable Mg signal above the IUVS threshold of 130 cm⁻³ at 90 km. If meteoric ablation injects the magnesium mainly as Mg atoms, then the lack of a pronounced Mg layer cannot be explained in terms of the known chemistry of Mg. This is because the very unreactive Mg atoms should only react with O₃ or O₂⁺ in the Mars atmosphere below 100 km (Table S1), and neither of these reactants has a high concentration⁶. One possibility is that when Mg atoms evaporate during ablation, they are initially travelling at

hyperthermal velocities ($> 5 \text{ km s}^{-1}$) and therefore have more than enough impact energy to react with CO_2 to make $\text{MgO} + \text{CO}$ (a reaction that is endothermic by 272 kJ mol^{-1} ³⁷). In the model runs discussed below, it is assumed that ablation produces 90% MgO below 100 km, and 90% of Mg^+ at higher altitudes (which is where the faster-moving meteoroids ablate, leading to a greater probability of ionization³⁷).

The model was used to test the effect of varying α on the modeled Mg^+ and Mg layers. The results of setting $\alpha = 0.01$ and 1 are illustrated in Figures S3 and S4, respectively. With the small value of α most of the MgCO_3^+ dissociates to Mg upon electron recombination. The enhanced Mg then produces more Mg^+ below 90 km, so that the underside of the Mg^+ layer is then in very good agreement with the IUVS observations, as is the case for the rest of the layer above 90 km (Figure S3). For this simulation, an Mg ablation flux of $6900 \text{ cm}^{-2} \text{ s}^{-1}$ is required. Note, however, that the Mg layer now peaks at 490 cm^{-3} , a factor of 3.8 above the IUVS detection threshold.

In contrast when $\alpha = 1$, dissociative recombination produces MgO which rapidly recombines with CO_2 to make MgCO_3 , and this in turn reacts with H_2O to form the stable Mg reservoir $\text{Mg}(\text{OH})_2$ ³⁷. As shown in Figure S4, the Mg layer is now reduced to below the IUVS threshold. However, the underside of the Mg^+ layer cuts off more sharply than observed – though that is a less important criterion than the absence of detectable Mg . For this simulation, the Mg ablation flux needs to be increased to $10900 \text{ cm}^{-2} \text{ s}^{-1}$.

Extrapolating globally the ablation input of Mg, distinct from unmelted micrometeorites and cosmic spherules, would then be $0.057 \text{ tonnes sol}^{-1}$. Unmelted material can be determined from our understanding of the terrestrial atmosphere, where a recent study of the contributions of cosmic dust from Jupiter Family Comets, Asteroids and Long Period Comets concluded that overall 1 tonne of Mg ablated from 43 tonnes of dust ²². Translating this ratio to Mars where the fraction ablating is slightly lower because of the reduced entry velocity of the dust particles ²⁰, 1 tonne of Mg ablates from about 55 tonnes of dust. This implies that the total dust input at Mars is $3.2 \text{ tonnes sol}^{-1}$.

Data Availability

The data have been publicly archived at the Planetary Atmospheres node of the Planetary Data System (PDS). Data products used herein are of the form: periapse[**]leve11b.

References

- 29 Risberg, P. "THE SPECTRUM OF SINGLY-IONIZED MAGNESIUM, MG-II." *Arkiv for Fysik* 9.5: 483-494 (1955)
- 30 A'Hearn, M. F., J. T. Ohlmacher, and D. G. Schleicher, Technical Report: TR AP83-044 (College Park: University of Maryland), 1983
- 31 A'Hearn M., Personal Communication
- 32 Rosenqvist, J. & Chassefiere, E. A Re-examination of the relationship between eddy mixing and O₂ in the Martian middle atmosphere. *J. Geophys. Res.* **100**, 5541-5551 (1995).
- 33 Izakov, M. N. Martian upper atmosphere structure from the Viking spacecraft experiments. *Icarus* **36**, 189-197 (1978).
- 34 Pesnell, W. D. & Grebowsky, J. Meteoric magnesium ions in the Martian atmosphere. *J. Geophys. Res.* **105**, 1695-1707 (2000).
- 35 Rodrigo, R., Garcia-Alvarez, E., Lopez-Gonzalez, M. J. & Lopez-Moreno, J. J. A non steady-state one-dimensional theoretical model of Mars neutral atmosphereic

- composition between 30 km and 200 km. *J. Geophys. Res.* **95**, 14795-14810 (1990).
- 36 Whalley, C. L., Gomez Martin, J. C., Wright, T. G. & Plane, J. M. C. A kinetic study of Mg^+ and Mg-containing ions reacting with O_3 , O_2 , N_2 , CO_2 , N_2O and H_2O : implications for magnesium ion chemistry in the upper atmosphere. *Phys. Chem. Chem. Phys.* **13**, 6352-6364, doi:10.1039/c0cp02637a (2011).
- 37 Plane, J. M. C. & Whalley, C. L. A New Model for Magnesium Chemistry in the Upper Atmosphere. *J. Phys. Chem. A* **116**, 6240-6252, doi:10.1021/jp211526h (2012).
- 38 Vondrak, T., Woodcock, K. R. I. & Plane, J. M. C. A kinetic study of the reactions of Fe^+ with N_2O , N_2 , O_2 , CO_2 and H_2O , and the ligand-switching reactions $\text{Fe}^+ \cdot \text{X} + \text{Y} \rightarrow \text{Fe}^+ \cdot \text{Y} + \text{X}$ ($\text{X} = \text{N}_2$, O_2 , CO_2 ; $\text{Y} = \text{O}_2$, H_2O). *Phys. Chem. Chem. Phys.* **8**, 503-512, doi:10.1039/b508922k (2006).
- 39 Plane, J. M. C. & Helmer, M. Laboratory study of the reactions $\text{Mg} + \text{O}_3$ and $\text{MgO} + \text{O}_3$ - Implications for the chemistry of magnesium in the upper atmosphere. *Faraday Disc.*, 411-430 (1995).
- 40 Rollason, R. J. & Plane, J. M. C. A kinetic study of the reactions of MgO with H_2O , CO_2 and O_2 : implications for magnesium chemistry in the mesosphere. *Phys. Chem. Chem. Phys.* **3**, 4733-4740 (2001).
- 41 Rutherford, J. A., Mathis, R. F., Turner, B. R. & Vroom, D. A. Formation of Magnesium Ions by Charge Transfer. *J. Chem. Phys.* **55**, 3785 (1971).
- 42 Rowe, B. R., Fahey, D. W., Ferguson, E. E. & Fehsenfeld, F. C. Flowing afterflow studies of gas phase magnesium ion chemistry. *J. Chem. Phys.* **75**, 3325-3328 (1981).
- 43 Florescu-Mitchell, A. I. & Mitchell, J. B. A. Dissociative recombination. *Phys. Lett.* **430**, 277-374 (2006).
- 44 Badnell, D. R. Radiative Recombination Data for Modeling Dynamic Finite-Density Plasmas. *Astrophys. J. Suppl. Ser.* **167**, 334-342 (2006).
- 45 Kelley, M., Farnham, T., Bodewits, D., Tricarico, P. & Farnocchia, D. A STUDY OF DUST AND GAS AT MARS FROM COMET C/2013 A1 (SIDING SPRING). *Astrophysical J Lett* **792**, L16 (2014)
- 46 Vaubaillon, J. Personal communication
- 47 Christou, A., and Vaubaillon, J. "Numerical modeling of cometary meteoroid streams encountering Mars and Venus." *Solar System Bodies. NASA/CP-* 2011 (2011)

- 48 Christou, A., and Buerle, K. "Meteoroid streams at Mars: possibilities and implications." *Planetary and Space Science* 47.12 (1999): 1475–1485
- 49 Christou, A. "PREDICTING MARTIAN AND VENUSIAN METEOR SHOWER ACTIVITY." *Earth, Moon, and Planets* 95.1-4 (2006): 425–431
- 50 Christou, A. "Annual meteor showers at Venus and Mars: lessons from the Earth." *Monthly Notices of the Royal Astronomical Society* 402.4 (2010): 2759–2770